chemosensors

MDPI

Supporting Information

Carbon Dots Fluorescence-Based Colorimetric Sensor for Sensitive Detection of Aluminum Ions with a Smartphone

Wei Wei[1,†], Juan Huang[1,†], Wenli Gao[1], Xiangyang Lu[2,*] and Xingbo Shi[1,2,*]

[1] Laboratory of Micro & Nano Biosensing Technology in Food Safety, Hunan Provincial Key Laboratory of Food Science and Biotechnology, College of Food Science and Technology, Hunan Agricultural University, Changsha, 410128, China; shixingbo123@aliyun.com (X.B.S.)
[2] College of Bioscience and Biotechnology, Hunan Agricultural University, Changsha, 410128, China; xiangyangcn@163.com (X.Y.L.); shixingbo123@aliyun.com (X.B.S.)
* Correspondence: xiangyangcn@163.com (X.Y.L.); shixingbo123@aliyun.com (X.B.S.); Tel.: +86-731-84673517(X.S.)
† These authors contributed equally to this work.

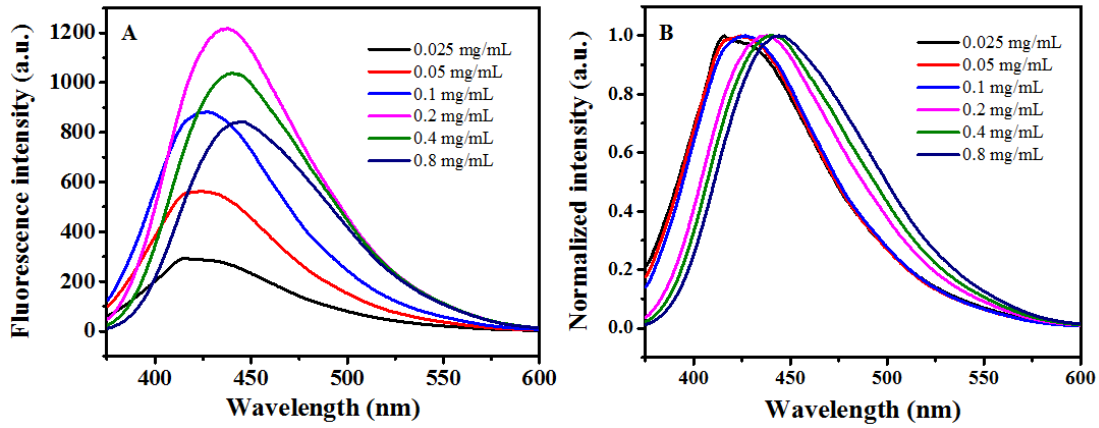

Figure S1. (**A**) Fluorescence spectra and (**B**) normalized fluorescence spectra of CDs with different concentrations.

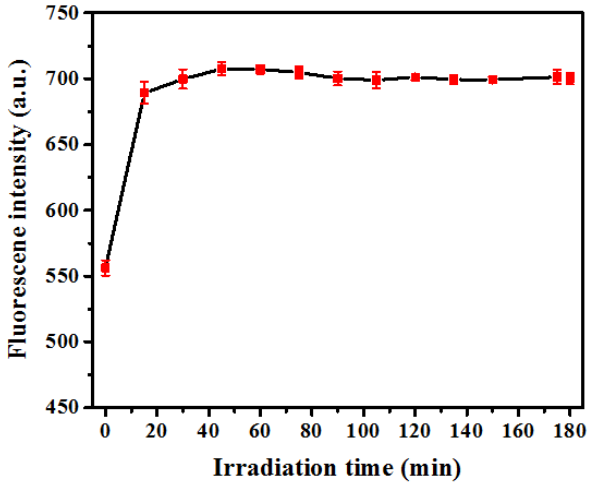

Figure S2. Anti-photobleaching property of the CDs when irradiated under UV lamp for 3 hours.

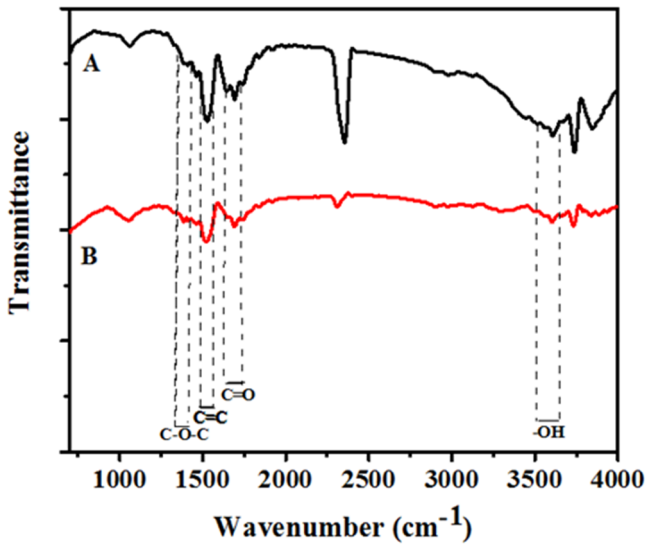

Figure S3. The FTIR spectra of CDs (A) before and (B) after irradiation at 360 nm UV lignt for 15 mins.

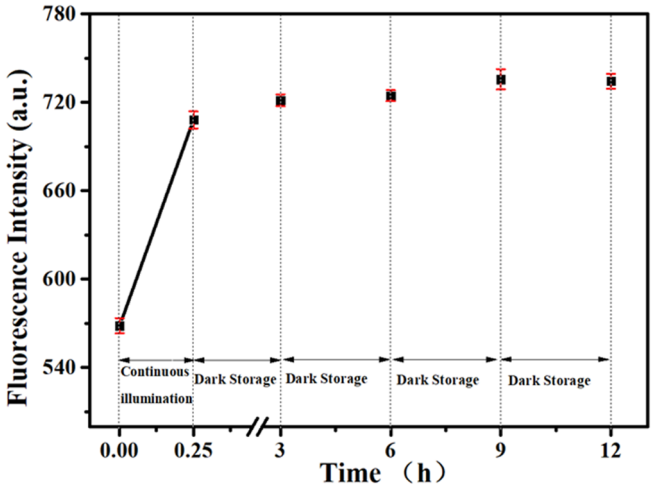

Figure S4. The fluorescence intensity of CDs at different dark storage time interval when irradiated under UV lamp for 15 min once.

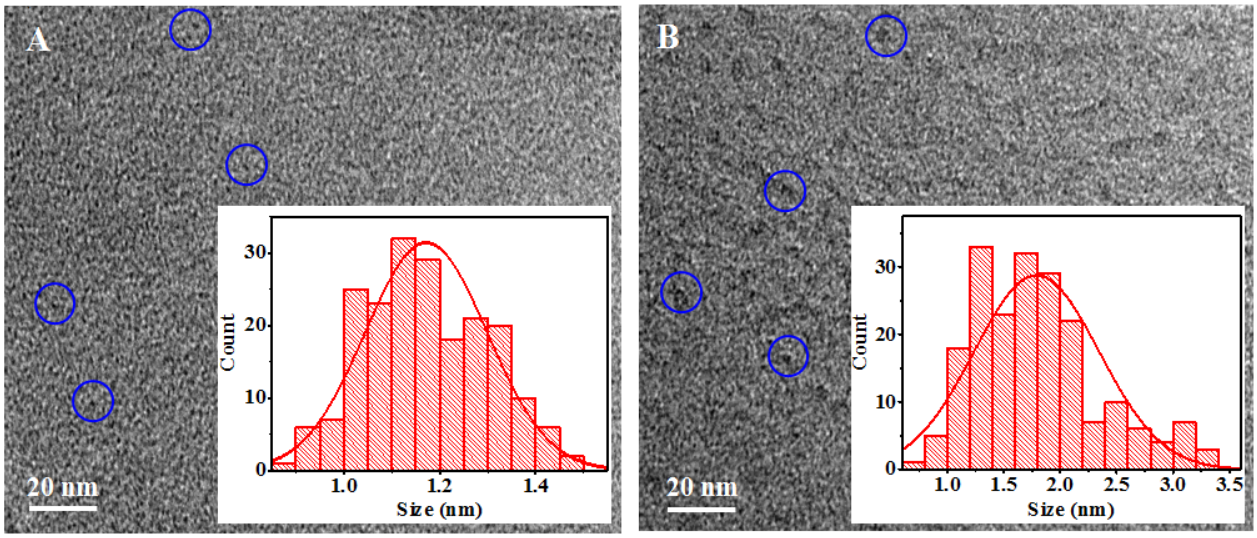

Figure S5. TEM images of (A) CDs, (B) CDs with the addition of Al^{3+} (7.69 mM), the inset shows the distribution histogram of the average diameter of CDs and CDs- Al^{3+}, respectively.

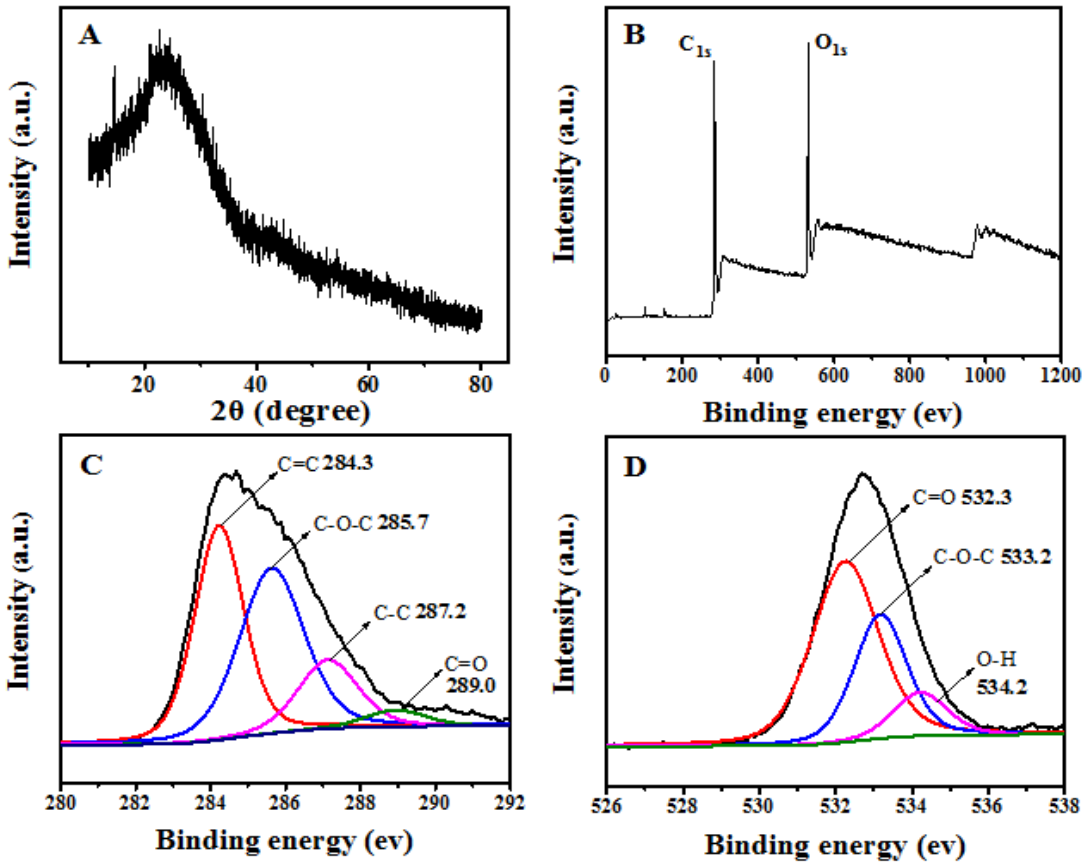

Figure S6. XRD and XPS spectrum of the CDs.

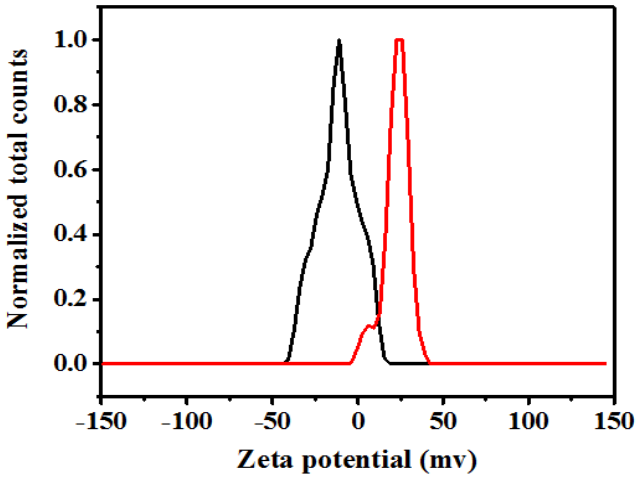

Figure S7. Zeta potential of the CDs and the CDs-Al^{3+} (7.69 mM).

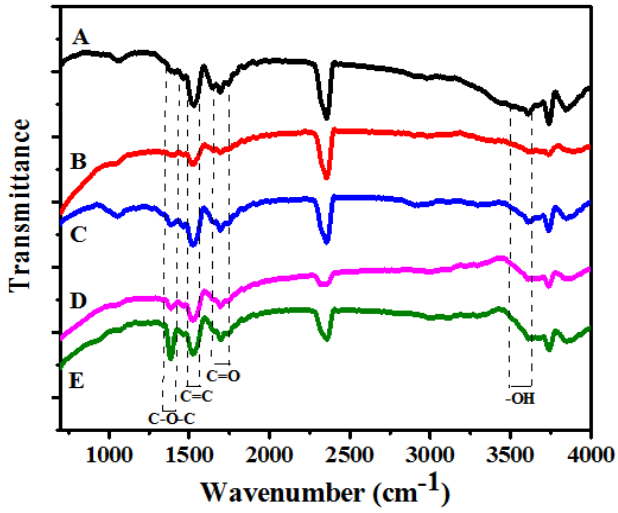

Figure S8. FTIR spectra of (**A**) CDs, (**B-E**) CDs with the addition of different concentration of Al^{3+} (7.69 μM, 76.9 μM, 769μM, 7.69 mM).

Figure S9. Fluorescence spectra (**A**) and I_{500}/I_{420} (**B**) of CDs after adding 76.92 μM Al^{3+} at the pH from 4.0 to 9.0.

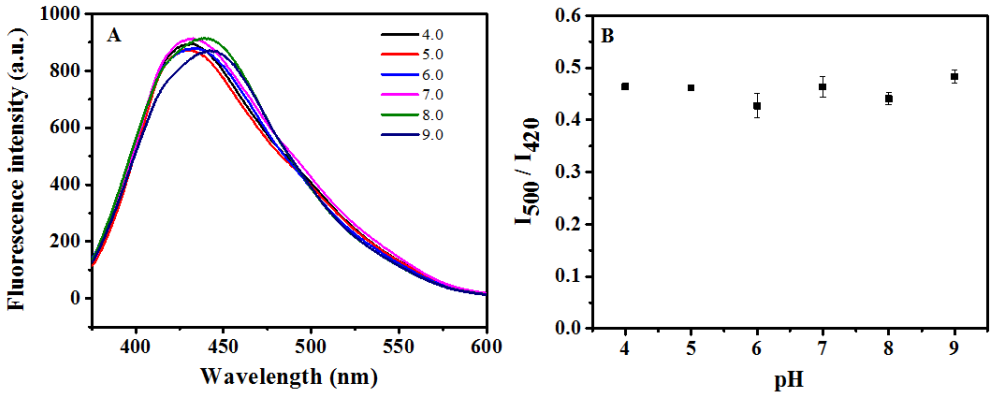

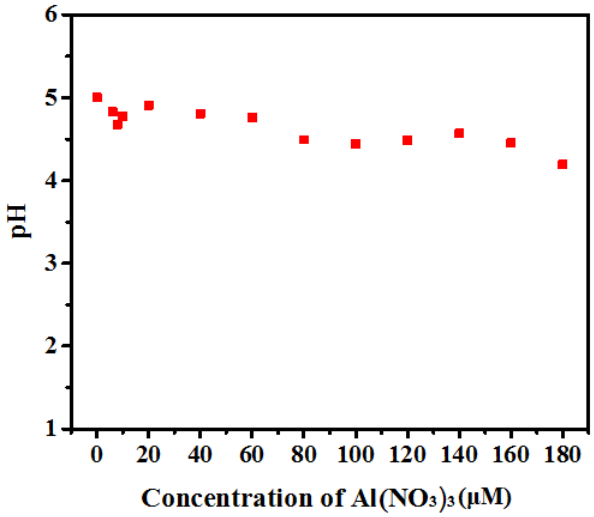

Figure S10. the pH value of different concentrations of $Al(NO_3)_3$ in acetic-acetate buffer solution (pH 5.0).

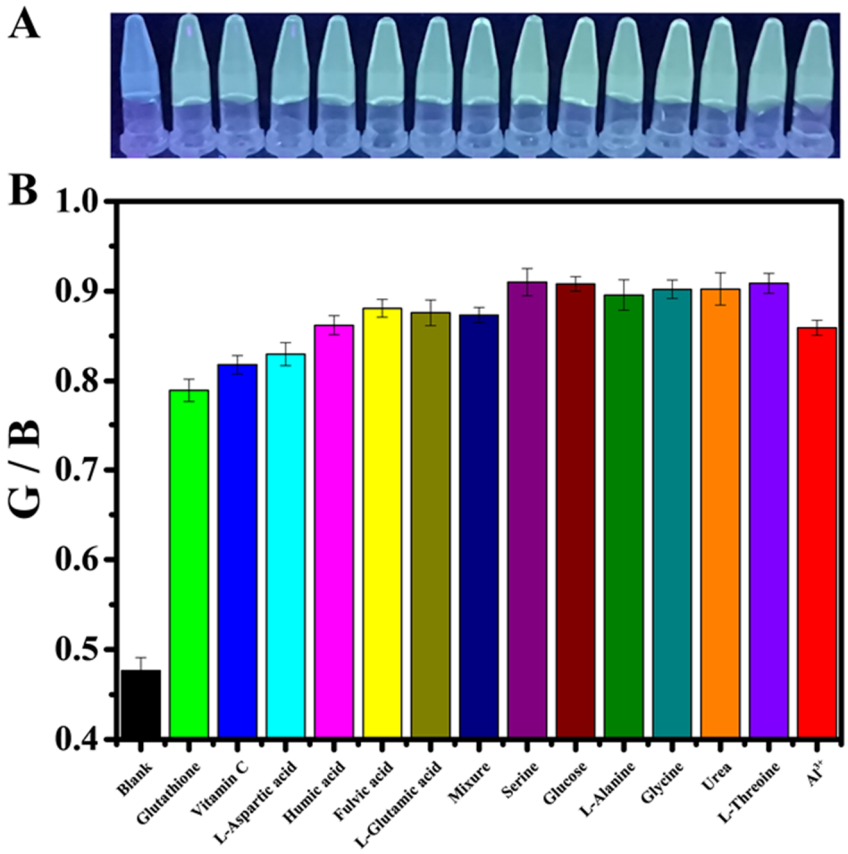

Figure S11. Evaluation of the interference from various small molecules in the RGB method. (**A**) images of the CDs-Al^{3+} (307.69 μM) solution upon the addition of different small molecule and the mixture of above small molecules obtained with a smartphone under a 360 nm UV lamp. (**B**) G/B value responses to the different small molecule (307.69 μM glutathione, vitamin C, L-aspartic, fulvic acid, L-glutamic, serine, glucose, L-alanine, glycine, urea, L-threoine and 247 μg/mL humic acid).

Table S1. Comparison among different methods used in the Al^{3+} detection.

Platform/Probe	Mechanism	Liner range/M	Limit of detection/M	Ref
Fluorescence method/HL	ESIPT and PET	---	4.0×10^{-6}	1
Fluorescence method/BOS	CHEF	---	1.855×10^{-6}	2
Fluorescence method /L1	CHEF	---	8.2×10^{-7}	3
Fluorescence method/CDs	Surface passivation	0-1.0×10^{-5}	3.9×10^{-7}	4
Fluorescence method/L2	PET	---	7.5×10^{-7}	5
Fluorescence method/HBTP	ESIPT and CHEF	0-1.2×10^{-5}	6.72×10^{-8}	6
Fluorescence method/Cys-CuNCs	AIE	1.0×10^{-6}-1.0×10^{-6}	2.67×10^{-8}	7
Fluorescence method/(R)-1	N and O atoms of (R)-1 interacting with Al^{3+}	---	1.4×10^{-8}	8
Fluorescence method/Hmppc	CHEF	1.0×10^{-6}-4.0×10^{-6}	1.2×10^{-9}	9
Fluorescence method/L3	PICT and TICT	1.75×10-9-3.3×10^{-8}	1.62×10^{-10}	10
RGB method/CP-ATP	Interaction of ATP with Al^{3+}	4.0×10^{-6}-4.0×10^{-4}	3.7×10^{-6}	11
Colorimetric method/RB/bis-PDA	Interaction of RB with Al^{3+}	0-9.0×10^{-5}	1.8×10^{-6}	12
Colorimetric method/IL-AuNPs	N atoms of IL interacting with Al^{3+}	---	1.0×10^{-6}	13
Colorimetric method/PQTEG	N atoms of PQTEG interacting with Al^{3+}	---	8.0×10^{-7}	14
Colorimetric method/MMT–AuNP	N atoms of MMT–AuNP interacting with Al^{3+}	1.0×10^{-6}-1.0×10^{-5}	5.3×10^{-7}	15
Colorimetric method/TTP–AuNPs	Triazole–ether interacting with Al^{3+}	5.0×10^{-7}-5.0×10^{-6}	1.8×10^{-8}	16
Colorimetric method/H	O atoms of H interacting with Al^{3+}	0-3.0×10^{-5}	1.42×10^{-8}	17
Colorimetric method/J-AgNPs	O atoms of J-AgNPs interacting with Al^{3+}	1.0×10^{-7}-1.0×10^{-5}	1.0×10^{-8}	18
Fluorescence method/CDs	O atoms of CDs interacting with Al^{3+}	1.54×10^{-7}-3.85×10^{-5}	1.138×10^{-7}	This work
RGB method/CDs	O atoms of CDs interacting with Al^{3+}	1.54×10^{-5}-1.54×10^{-4}	5.55×10^{-6}	This work

HL: 2-hydroxy-1-naphthylaldehyde nicotinoyl hydrazone

BOS: rhodamine B-based chromo-fluorogenic probe

L1:8-formyl-7-hydroxyl-4-methyl coumarin–(20-methylquinoline-4-formyl) hydrazone

L2:2-hydroxy-5-(4-nitrophenyl)diazenyl) benzaldehyde-appended rhodamine based scaffold

HBTP: pyridine conjugated hydroxybenzothiazole

Cys-CuNCs: Cysteamine-capped copper nanoclusters

(R)-1: (2R,20R)-2,2'-((1,3-phenylenebis(methylene))bis((pyren-1-ylmethyl)azanediyl))bis(2-phenylethan-1-ol)

Hmppc: 5-methyl-1-pyridin-2-yl-1H-pyrazole-3-carboxylic acid (1-pyridin-2-yl-ethylidene)-hydrazide

L3: (5-[(4-diethylamino-2-hydroxy-benzylidene)-amino]-1H-pyrimidine-2, 4-dione)

CP-ATP: copolymer-ATP

RB/bis-PDA film: rhodamine B-functionalized bis-polydiacetylene film

IL-AuNPs: 1-ethyl-3-methylimidazolium thiocyanate-coated gold nanoparticles

PQTEG:(2-(2-(2-hydroxyethoxy)ethoxy)ethyl 8-propoxyquinoline-2-carboxylate)

MMT–AuNP: 5-mercaptomethyltetrazole- gold nanoparticles

TTP–AuNPs: triazole–ether functionalized gold nanoparticles

H: the organic-inorganic nanohybrid by immobilization of AuNPs on organic nanoparticles

J-AgNPs: the bifunctional Jamun stabilized silver nanoparticles

ESIPT: excited state intramolecular proton transfer mechanism; PET: photo-induced electron transfer; CHEF: chelation-enhanced fluorescence; AIE: aggregate-induced emission; PICT: normal planar intramolecular charge transfer; TICT: twisted intramolecular charge transfer.

References

1. Qin, J.C.; Yang, Z.Y.; Yang, P. Recognition of Al^{3+} based on a naphthalene-based "off-on" chemosensor in near 100% aqueous media. *Inor. Chim. ACTA* **2015**, *432*, 136-141. https://doi.org/10.1016/j.ica.2015.03.029.

2. Leng, X.; Jia, X.; Qiao, C.F.; Xu, W.F.; Ren, C.T.; Long, Y.; Yang, B.Q. Synthesis, characterization and Al^{3+} sensing application of a new chromo-fluorogenic chemosensor. *J. Mol. Struct*. **2019**, *1193*, 69-75. https://doi.org/10.1016/j.molstruc.2019.05.032.

3. Qin, J.C.; Li, T.R.; Wang, B.D.; Yang, Z.Y.; Fan, L. Fluorescent sensor for selective detection of Al^{3+} based on quinoline–coumarin conjugate. *Spectrochim. ACTA A* **2014**, *133*, 38-43. https://doi.org/10.1016/j.saa.2014.05.033.

4. Sun, X.Y.; Wu, L.L.; Shen, J.S.; Cao, X.G.; Wen, C.J.; Liu, B.; Wang, H.Q. Highly selective and sensitive sensing for Al^{3+} and F^- based on green photoluminescent carbon dots. *RSC Adv*. **2016**, *6*, 97346-97351. https://doi.org/10.1039/c6ra19370f.

5. Gupta, V.K.; Singh, A.K.; Kumawat, L.K. Thiazole Schiff base turn-on fluorescent chemosensor of Al^{3+} ion. *Sensor. Actuat. B-Chem*. **2014**, *195*, 98-108. https://doi.org/10.1016/j.snb.2013.12.092.

6. Das, S.; Goswami, S.; Aich, K.; Ghoshal, K.; Quah, C.K.; Bhattacharyya, M.; Fun, H.K. ESIPT and CHEF based highly sensitive and selective ratiometric sensor for Al^{3+} with imaging in human blood cell. *New J. Chem*. **2015**, *39*, 8582-8587. https://doi.org/ 10.1039/c5nj01468a.

7. Boonmee, C.; Promarak, V.; Tuntulani, T.; Ngeontae, W. Cysteamine-capped copper nanoclusters as a highly selective turn-on fluorescent assay for the detection of aluminum ions. *Talanta* **2018**, *178*, 796-804. https://doi.org/10.1016/j.talanta.2017.10.006.

8. Prabhu, J.; Velmurugan, K.; Raman, A.; Duraipandy, N.; Kiran, M.S.; Easwaramoorthi, S.; Tang, L.J.; Nandhakumar, R. Pyrene-phenylglycinol linked reversible ratiometric fluorescent chemosensor for the detection of aluminium in nanomolar range and its bio-imaging. *Anal. Chim. ACTA* **2019**, *1090*, 114-124. https://doi.org/10.1016/j.aca.2019.09.008.

9. Naskar, B.; Das, K.; Mondal, R.R.; Maiti, D.K.; Requena, A.; Ceron, C.J.P.; Prodhan, C.; Chaudhuri, K.; Goswami, S. A new fluorescence turn-on chemosensor for nanomolar detection of Al^{3+} constructed from pyridine-pyrazole system. *New J. Chem*. **2018**, *42*, 2933-2941. https://doi.org/10.1039/c7nj03955g.

10. Upadhyay, K.K.; Kumar, A. Pyrimidine based highly sensitive fluorescent receptor for Al^{3+} showing dual signalling mechanism. *Org. Biomol. Chem*. **2010**, *8*, 4892-4897. https://doi.org/10.1039/c0ob00171f.

11. Tu, M.C.; Rajwar, D.; Ammanath, G.; Alagappan, P.; Yildiz, U.H.; Liedberg, B. Visual detection of Al^{3+} ions using conjugated copolymer-ATP supramolecular complex. *Anal. Chim. ACTA* **2016**, *912*, 105-110. https://doi.org/10.1016/j.aca.2015.12.002.

12. Wang, H.; Han, S.H. Bis-ratiometric absorbance detection of Al(III) in the rhodamine B-functionalized bis-polydiacetylene film. *Chem. Pap.* **2017**, *71*, 2129-2137. https://doi.org/10.1007/s11696-017-0205-9.

13. Chen, W.W.; Jia, Y.X.; Feng, Y.; Zheng, W.S.; Wang, Z.; Jiang, X.Y. Colorimetric detection of Al(III) in vermicelli samples based on ionic liquid group coated gold nanoparticles. *RSC Adv*. **2015**, *5*, 62260-62264. https://doi.org/10.1039/c5ra09099g.

14. Jisha, B.; Resmi, M.R.; Maya, R.J.; Varma, R.L. Colorimetric detection of Al(III) ions based on triethylene glycol appended 8-propyloxy quinoline ester. *Tetrahedron Lett*. **2013**, *54*, 4232-4236. https://doi.org/10.1016/j.tetlet.2013.05.134.

15. Xue, D.S.; Wang, H.Y.; Zhang, Y.B. Specific and sensitive colorimetric detection of Al^{3+} using 5-mercaptomethyltetrazole capped gold nanoparticles in aqueous solution. *Talanta* **2014**, *119*, 306-311. https://doi.org/10.1016/j.talanta.2013.11.012.

16. Chen, Y.C.; Lee, I.L.; Sung, Y.M.; Wu, S.P. Colorimetric detection of Al^{3+} ions using triazole–ether functionalized gold nanoparticles. *Talanta* **2013**, *117*, 70-74. https://doi.org/10.1016/j.talanta.2013.08.054.

17. Kaur, R.; Kaur, N.; Kuwar, A.; Singh, N. Colorimetric sensor for detection of trace level Al(III) in aqueous medium based on organic-inorganic nanohybrid. *Chem. Phys. Lett*. **2019**, *722*, 140-145. https://doi.org/10.1016/j.cplett.2019.03.014.

18. Painuli, R.; Joshi, P.; Kumar, D. Cost-effective synthesis of bifunctional silver nanoparticles for simultaneous colorimetric detection of Al(III) and disinfection. *Sensor. Actuat. B-Chem*. **2018**, *272*, 79-90. https://doi.org/10.1016/j.snb.2018.05.131.

Publisher's Note: MDPI stays neutral with regard to jurisdictional claims in published maps and institutional affiliations.

© 2020 by the authors. Submitted for possible open access publication under the terms and conditions of the Creative Commons Attribution (CC BY) license (http://creativecommons.org/licenses/by/4.0/).